Biomacromolecules

ARTICLE

pubs.acs.org/Biomac

Synthesis of Amphiphilic Alternating Polyesters with Oligo(ethylene glycol) Side Chains and Potential Use for Sustained Release Drug Delivery

Wei Wang,[†,§] Jianxun Ding,[†,‡,§] Chunsheng Xiao,[†,‡] Zhaohui Tang,[†] Di Li,[†] Jie Chen,[†] Xiuli Zhuang,[*,†] and Xuesi Chen[†]

[†]Key Laboratory of Polymer Ecomaterials, Changchun Institute of Applied Chemistry, Chinese Academy of Sciences, Changchun 130022, P. R. China

[‡]Graduate University of Chinese Academy of Sciences, Beijing 100039, P. R. China

Supporting Information

ABSTRACT: Novel amphiphilic alternating polyesters, poly((*N*-phthaloyl-L-glutamic anhydride)-*co*-(2-(2-(2-methoxyethoxy)ethoxy)methyl)oxirane) (P(PGA-*co*-ME$_2$MO)), were synthesized by alternating copolymerization of PGA and ME$_2$MO. The structures of the synthesized polyesters were characterized by ^{1}H NMR, ^{13}C NMR, FT-IR, and GPC analyses. Because of the presence of oligo(ethylene glycol) (OEG) side chains, the polyesters could self-assemble into thermosensitive micelles. Dynamic light scattering (DLS) showed that these micelles underwent thermoinduced size decrease without intermicellar aggregation. In vitro methyl thiazolyl tetrazolium (MTT) assay demonstrated that the polyesters were biocompatible to Henrietta Lacks (HeLa) cells, rendering their potential for drug delivery applications. Two hydrophobic drugs, rifampin and doxorubicin (DOX), were loaded into the polyester micelles and observed to be released in a zero-order sustained manner. The sustained release could be accelerated in lower pH or in the presence of proteinase K, due to the degradation of the polyester under these conditions. Remarkably, in vitro cell experiments showed that the polyester micelles accomplished fast release of DOX inside cells and higher anticancer efficacy as compared with the free DOX. With enhanced stability during circulation condition and accelerated drug release at the target sites (e.g., low pH or enzyme presence), these novel polyesters with amphiphilic structures are promising to be used in sustained release drug delivery systems.

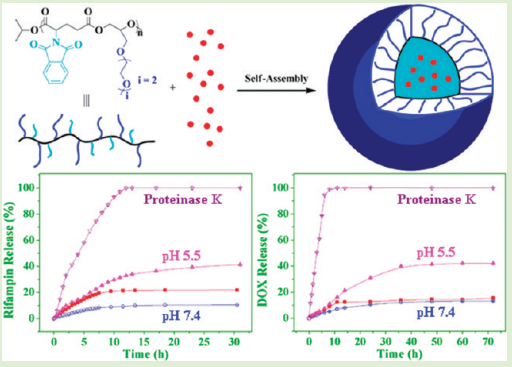

INTRODUCTION

It is well known that amphiphilic block copolymers can self-assemble into various morphologies,[1−5] such as vesicles[6,7] and micelles,[8] depending on the type of selective solvent, the polymer concentration, and the chain structure. Not only the amphiphilic block copolymers but also a number of polymers with amphiphilic structures are capable of providing diverse self-assembled structures.[9−11] Thayumanavan et al. developed a molecular design based on homopolymers in which both the hydrophilic and hydrophobic moieties are incorporated within one structure unit.[12] Such homopolymers can form both micelle and inverse micelle assemblies depending on the solvent environment. Amphiphilic graft copolymers consisting of hydrophobic backbones and hydrophilic side chains or vice versa are another kind of interesting materials that can self-assemble into various morphologies. For instance, Huang et al. was reported to synthesize well-defined amphiphilic copolymers with hydrophilic poly(acrylic acid) (PAA) backbones and hydrophobic poly(propylene oxide) (PPO) side chains, which can self-assemble into micelles.[13] The biodegradable and biocompatible polypeptide can also be introduced as the hydrophobic backbone for its potential biomedical applications. Chen and coworkers reported that the poly(L-glutamate)s (PLG) were grafted with thermosensitive poly(2-(2-methoxyethoxy)ethyl methacrylate) (PMEO$_2$MA) or oligo(2-(2-(2-methoxyethoxy)ethoxy)ethyl methacrylate) (OMEO$_3$MA) chains through atom transfer radical polymerization.[14,15] The resultant copolymers can form micellar aggregates in aqueous solution with α-helical polypeptide cores and thermosensitive PMEO$_2$MA or OMEO$_3$MA shells. These micelles showed decreased size at elevated temperature without intermicellar aggregation, which was attractive for drug delivery application.

Among all of the above-mentioned amphiphilic assemblies, the micelles self-assembled in aqueous solution have many potential applications in biomedical fields, such as controlled drug release[16,17] and gene delivery,[18,19] because of their biodegradability[20,21] and biocompatibility.[22] The self-assembled micelles consist of the hydrophobic cores away from the water and the hydrophilic shells extending into the water. These self-assembled micelles have attracted significant attention as ideal drug delivery systems,[23] which are more

Received: January 26, 2011
Revised: June 3, 2011
Published: June 08, 2011

Scheme 1. Synthesis Pathway for PGA Monomer

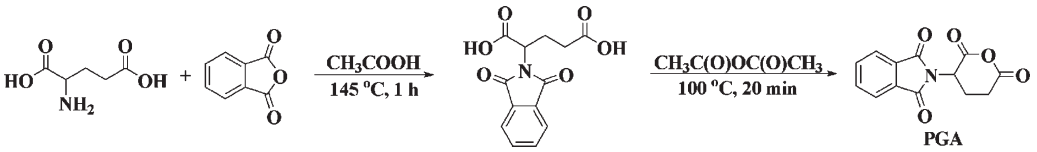

effective to increase the apparent solubility of the hydrophobic drug and the benefit of drug and thereby decrease the side effect.[24] However, the burst drug release from the micelles limits the application of almost all the micelle-based drug delivery systems.[25−27]

To overcome this limitation for drug delivery application, the novel alternating polyesters with hydrophobic *N*-phthaloyl groups in the polyester backbone and hydrophilic oligo(ethylene glycol) (OEG) side chains were synthesized in the present work. The strong hydrophobic interaction between *N*-phthaloyl groups and drugs can weaken the burst drug release from micelles.[28] The OEG side chains can resist nonspecific protein adsorption (i.e., nonfouling properties) in the complicated in vivo circumstance.[29] The micelles with OEG shells will be advantageous in drug delivery. In addition, polymers bearing OEG side chains, such as poly(oligo(ethylene glycol) acrylate) (POEGMA), are used as a class of thermosensitive materials.[30,31] Accordingly, the self-assembled polyester micelles with OEG shells were also thermosensitive and showed thermoinduced size decrease without intermicellar aggregation in aqueous solution. This property would further compress the micelles at the physiological temperature, and less burst release could be expected. Therefore, we anticipated that these amphiphilic alternating polyesters would show promising use in the sustained release drug delivery. For this purpose, rifampin and doxorubicin (DOX) were loaded into the micelles, and the release behaviors were monitored with an ultraviolet−visible (UV−vis) spectrophotometer under different conditions. In addition, in vitro cell experiments revealed that these polyester micelles accomplished fast release of DOX inside cells and higher anticancer efficacy as compared with the free DOX control.

EXPERIMENTAL SECTION

Materials. L-Glutamic acid (99%, Shanghai Huishi), phthalic anhydride (Beijing Chemical Works), tetrabutylammonium hydrogen sulfate (99%, Aldrich), and 2-(2-methoxyethoxy)ethanol (98%, Aldrich) were used without further purification. Aluminum isopropoxide (AIP) and acetic anhydride (Sinopharm Chemical Reagen) were distilled before used. Rifampin and doxorubicin hydrochloride (DOX·HCl) were purchased from Zhejiang Hisun Pharmaceutical and used as received. All other reagents and solvents were purchased from Sinopharm Chemical Reagent, China and used as obtained.

Synthesis of 2-(1,3-Dioxoisoindolin-2-yl)pentanedioic Acid (Scheme 1). Phthalic anhydride (70 g, 0.47 mol), glacial acetic acid (150 mL), and L-glutamic acid (74 g, 0.5 mol)) were added to a 500 mL round-bottomed flask. The mixture was refluxed at 145 °C for 1 h. Afterward, the reaction mixture was filtrated to remove the insoluble substance. The filtrate was evaporated and then recrystallized from water to afford the product (yield: 85.0%). ^{1}H NMR (400 MHz, DMSO-d_6, ppm): 2.26−2.50 (m, 4H), 4.91 (m, 1H), 7.75−7.86 (m, 4H). FT-IR (KBr): Absorptions at 1777 cm^{-1}, 1712 cm^{-1} are the stretching of carbonyl groups from *N*-phthaloyl group (Supporting Information, Figure S1).

Synthesis of *N*-Phthaloyl-L-glutamic Anhydride (PGA) (Scheme 1). In a 250 mL flask, 2-(1,3-dioxoisoindolin-2-yl)pentanedioic acid (20 g, 0.36 mol) and freshly distilled acetic anhydride (40 mL) were heated to 100 °C until the solution turned clear and then were stirred for an additional 5 min at 100 °C. The solution was cooled and concentrated under vacuum. The resulting solid was washed with cold acetic anhydride and dry ether, and then dried under vacuum (yield: 73.0%). ^{1}H NMR (400 MHz, DMSO-d_6, ppm): 2.54−2.68 (m, 2H), 2.94−3.18 (m, 2H), 5.46 (m, 1H), 7.92 (m, 4H). FT-IR (KBr): Absorptions at 1840, 1800, and 1730 cm^{-1} are the stretching of carbonyl groups from *N*-phthaloyl group and anhydride ring (Supporting Information, Figure S2).

Scheme 2. Synthesis Pathway for ME$_2$MO Monomer

Synthesis of (2-(2-(2-Methoxyethoxy)ethoxy)methyl)oxirane (ME$_2$MO) (Scheme 2). Tetrabutylammonium hydrogen sulfate (TBAHS, 5 g, 0.02 mol), epichlorohydrin(90 g, 0.97 mol), and aqueous sodium hydroxide(36 g, 50 wt %) were mixed with vigorous stirring at 0 °C. Then, the 2-(2-methoxyethoxy)ethanol (36 g, 0.3 mol) was added dropwise. The solution was allowed to warm to room temperature and stirred for a further 3 h. Chloroform was added to extract the product and washed with brine to neutrality. The organic phase was dried with sodium sulfate for 24 h. After filtration, the filtrate was evaporated and followed by vacuum distillation (80 °C, 10 Pa) (yield: 70.0%). ^{1}H NMR (400 MHz, $CDCl_3$, ppm): 2.61 (q, 1H), 2.80 (t, 1H), 3.17 (m, 1H), 3.39 (s, 3H), 3.44 (q, 1H), 3.55−3.58 (m, 2H), 3.63−3.73 (m, 6H), 3.78, 3.81 (dd, 1H). FT-IR (KBr): 1112 cm^{-1}(υ_{C-O-C}), the stretching absorptions at 1108 and 910 cm^{-1} are the characteristic bands of the epoxide group (Supporting Information, Figure S3).

Synthesis of P(PGA-*co*-ME$_2$MO) (Scheme 3). As a typical procedure, PGA (3.67 g, 14.1 mmol), ME$_2$MO (2.5 g, 14.1 mmol), and AIP (0.04 g, 0.19 mmol) were mixed in a dry flask. The mixture was stirred in bulk at 120 °C for 24 h. The crude product was dissolved in chloroform and precipitated with *n*-hexane/ethyl ether (1/1, v/v). The yellow oily product was obtained after drying at 70 °C for 24 h under vacuum (yield: 75.0%, $M_{n,NMR}$, $M_{n,GPC}$, and M_w/M_n were listed in Table 1).

Preparation of P(PGA-*co*-ME$_2$MO) Micelles. In brief, 5.0 mg of polyester was dissolved in 1 mL of DMF, and the solution was allowed to stir at room temperature for 2 h. Then, to this solution, 2 mL of deionic water was added with a rate of 1.0 mL min^{-1} under gentle stirring. After standing for 3 h at room temperature, DMF was removed by dialysis using a dialysis bag (MWCO 3500 Da) against deionic water for 24 h to obtain the micelles.

Characterization. ^{1}H NMR and ^{13}C NMR spectra were recorded on a Bruker AV 400 NMR spectrometer in chloroform-*d* ($CDCl_3$) or dimethyl sulfoxide-d_6 (DMSO-d_6). FT-IR spectra were recorded on a Bio-Rad Win-IR instrument using the potassium bromide (KBr) method. Number- and weight-average molecular weights (M_w, M_n) and molecular weight distributions (PDI = M_w/M_n) were determined by gel permeation chromatography (GPC) using a series of linear Styragel columns (HT_3 and HT_4) and a Waters 515 HPLC pump, with OPTILAB DSP interferometric refractometer (Wyatt Technology) as the detectors. The eluent was chloroform at a flow rate of 1.0 mL min^{-1} at 40 °C. Monodispersed polystyrene standards purchased from Waters with a molecular weight range of

Scheme 3. Synthesis Pathway for P(PGA-*co*-ME$_2$MO)

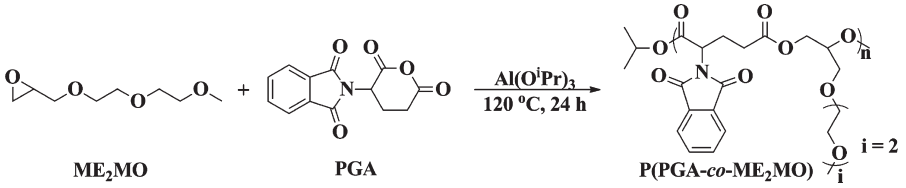

ME$_2$MO PGA P(PGA-*co*-ME$_2$MO)

Table 1. Characterizations of P(PGA-*co*-ME$_2$MO) Alternating Polyesters

polyester	feeding molar ratio of PGA(ME$_2$MO)/-O^{i}Pr	DP of P(PGA-*co*-ME$_2$MO)[a]	M_n[a]	M_n[b]	PDI[b]
P(PGA-*co*-ME$_2$MO)$_{23}$	25	23	10100	4800	1.14
P(PGA-*co*-ME$_2$MO)$_{47}$	50	47	20500	9900	1.16

[a] Determined by ^{1}H NMR. [b] Determined by GPC ($CHCl_3$ as eluent).

1310−55 100 were used to generate the calibration curve. Dynamic laser scattering (DLS) measurements were performed on a WyattQELS instrument with a vertically polarized He−Ne laser (DAWN EOS, Wyatt Technology). The scattering angle was fixed at 90°. Transmission electron microscopy (TEM) measurement was performed on a JEOL JEM-1011 transmission electron microscope with an accelerating voltage of 100 KV. A drop of the micelle solution (0.5 g L^{-1}) was deposited onto a 230 mesh copper grid coated with carbon and allowed to dry in air at 25 °C before measurements. Critical micelle concentration (CMC) was measured by fluorescence spectroscopy using pyrene as a probe on a Perkin-Elmer LS50B luminescence spectrometer at the detection wavelength (λ_{em}) of 390 nm. The CMC was obtained from the intersection of the tangent to the horizontal line of I_{335}/I_{332} with relative constant values and the diagonal line with rapidly increased I_{335}/I_{332} ratio.

Thermal Analyses. Thermal properties of the polyesters were examined by differential scanning calorimetry (DSC Q100, TA Instruments) under a N_2 atmosphere. The sample was heated from −35 to 80 °C at a rate of 10 °C min^{-1}, kept at 80 °C for 5 min and cooled to −35 °C at a rate of 10 °C min^{-1}. The data collection was carried out on the second heating run, and the glass-transition temperature (T_g) was taken to be the midpoint (the temperature corresponding to half of the endothermic shift).

In Vitro Enzymatic Degradation. The in vitro enzymatic degradation was performed at 37 °C in citric acid−disodium hydrogen phosphate buffer solution (CPBS, pH 7.4) containing proteinase K (2 μg mL^{-1}, 0.08 U mL^{-1}) and sodium azide (0.1 g L^{-1}). The concentration of the polyester was set at 0.5 g L^{-1}. At predetermined time intervals, samples were taken out and freeze-dried for GPC analyses.

Cytotoxicity Assay. The relative cytotoxicities of polyesters and drug-loaded polyester micelles were assessed with methyl thiazolyl tetrazolium (MTT) viability assay against Henrietta Lacks (HeLa) cells. The cells were seeded in 96-well plates at ∼20 000 cells per well in 100 μL of complete DMEM containing 10% fetal bovine serum, supplemented with 50 U mL^{-1} penicillin and 50 U mL^{-1} streptomycin, and incubated at 37 °C in 5% CO_2 atmosphere for 24 h, followed by removing culture medium and adding polyester solutions at different concentrations (0 to 0.1 g L^{-1}) or drug-loaded polyester micelles (0 to 10 mg L^{-1} DOX) (100 μL in complete DMEM medium). The cells were subjected to MTT assay after being incubated for another 24 h. The absorbance of the solution was measured on a Bio-Rad 680 microplate reader at 492 nm. Cell viability (%) was calculated by ($A_{sample}/A_{control}$) × 100, where A_{sample} and $A_{control}$ are denoted as absorbance of the sample well and control well (without polyester), respectively. Experiments were performed in triplicate.

In Vitro Drug Loading and Release. The polyester (50.0 mg) in 5.0 mL of DMF was mixed with 50.0 mg of rifampin or DOX·HCl (neutralized with one molar equivalent of triethylamine). The mixture was allowed to stand at room temperature for 2 h. Then, 5 mL of deionic water was added dropwise to this solution under stirring. The mixture was stirred at room temperature for 6 h, and the organic solvent was removed by dialysis against deionic water for 24 h to obtain the drug-loaded micelles. The solution was filtered and freeze-dried. The drug loading content (DLC%) and the drug loading efficiency (DLE %) of drug-loaded micelles were calculated by the following equations:

$$\mathrm{DLC}\% = \frac{\text{amount of drug in micelle}}{\text{amount of drug-loaded micelle}} \times 100\%$$

$$\mathrm{DLE}\% = \frac{\text{amount of drug in micelle}}{\text{total amount of drug for drug loading}} \times 100\%$$

In vitro drug release behaviors from the micelles were investigated in CPBS (pH 7.4). The weighed freeze-dried drug-loaded micelles were suspended in 5 mL of CPBS and introduced into a dialysis bag (MWCO 3500 Da). We initiated the release experiment by placing the end-sealed dialysis bag in 60 mL of CPBS at 37 °C with continuous shake at 70 rpm. At predetermined intervals, 5 mL of CPBS was taken out, and an equal volume of fresh CPBS was replenished. The amount of released drug was assayed by spectrophotometry at 480 nm using the standard curve method. The drug releases were also performed in CPBS (pH 7.4) with proteinase K (2 μg mL^{-1}, 0.08 U mL^{-1}) and sodium azide (0.1 g L^{-1}) and in CPBS at pH 5.5.

Intracellular DOX Release. The cellular uptake and intracellular release behaviors of DOX-loaded polyester micelles were determined by confocal laser scanning microscopy (CLSM) using HeLa cells. The cells were seeded in six-well plates at ∼200 000 cells per well in 2 mL of complete DMEM and cultured for 24 h, followed by removing culture medium and adding DOX-loaded polyester micelles at a final DOX concentration of 10 mg L^{-1} (2 mL in complete DMEM medium). Free DOX was used as the control. The cells were incubated with DOX-loaded micelles or free DOX for 0.5 or 2 h. Thereafter, the culture media were removed, and the cells were rinsed four times with PBS and fixed with 4% formaldehyde for 30 min at room temperature, and the cell nuclei were stained with 4′,6-diamidino-2-phenylindole (DAPI, blue). CLSM images of cells were obtained through confocal microscope (Olympus FluoView 1000).

RESULTS AND DISCUSSION

Synthesis of P(PGA-*co*-ME$_2$MO). The aliphatic polyesters can be directly synthesized by living ring-opening polymerization (ROP) of lactone monomers using covalent metal alkoxides or carboxylates as the catalysts.[33] AIP, one of the most widely used

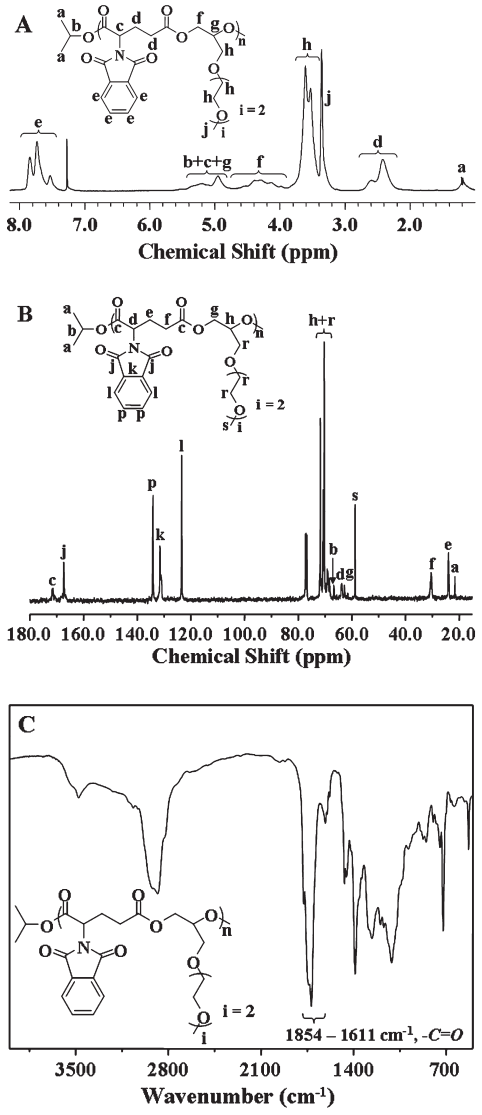

Figure 1. Typical ^{1}H NMR (in $CDCl_3$) (A), ^{13}C NMR (in $CDCl_3$) (B), and FT-IR (C) spectra of P(PGA-*co*-ME_2MO)$_{47}$.

catalysts, has been successfully applied in the ROP of ε-caprolactone, lactide, and cyclic phosphoester monomers through a coordination−insertion mechanism.[33,34] Recently, Hao et al. further investigated the use of AIP in the ring-opening alternative polymerization of succinic anhydride and functionalized epoxide.[32] In this work, we attempted to introduce natural glutamic acid to the polyester by using *N*-phthaloyl-glutamic anhydride (PGA) monomer. First, PGA and ME_2MO monomers were synthesized with the synthetic routes shown in Schemes 1 and 2, respectively.[32,35] The structures of PGA and ME_2MO monomers were confirmed by ^{1}H NMR and FT-IR spectra (Supporting Information, Figures S2 and S3, respectively). The polymerization was conducted in bulk at 120 °C with PGA/ME_2MO monomer molar feed ratio 1:1. The ^{1}H NMR signals (Figure 1A) clearly verified the composition of polyester generated from PGA and ME_2MO monomers. The molar composition of the two monomers in the resultant polyester was calculated to be 1:1 based on the integration of methylene d (2.22 to 2.82 ppm) from glutamic segment and methyl j (3.36 ppm) from OEG side chain. The homopolymerizations of PGA and ME_2MO were both not able to be initiated by AIP. The results indicated that

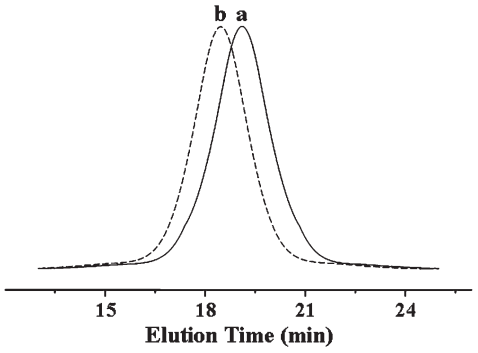

Figure 2. GPC chromatograms of P(PGA-*co*-ME_2MO)$_{23}$ (M_n = 4800, and PDI = 1.14) (a) and P(PGA-*co*-ME_2MO)$_{47}$ (M_n = 9900, and PDI = 1.16) (b).

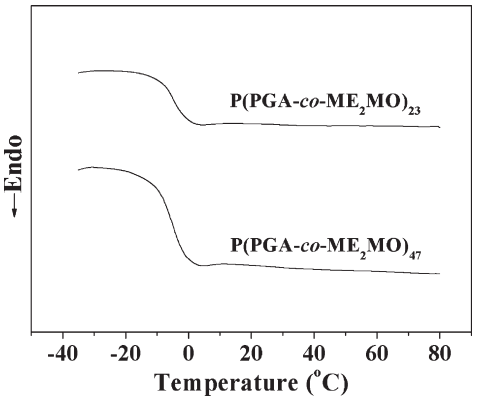

Figure 3. DSC thermograms of P(PGA-*co*-ME_2MO).

the copolymerization should be carried out alternatively in a strict way between PGA and ME_2MO monomers.[32] The degree of polymerization (DP, listed in Table 1) of P(PGA-*co*-ME_2MO) was calculated by comparing the integrated area of peak d or j with that of the signal at 1.19 ppm (a) assigned to methyl protons of isopropyloxy end group. The ^{13}C NMR spectrum (Figure 1B) confirmed the polyester structure. The signal at 171.6 ppm was assigned to the ester bond from backbone. FT-IR (Figure 1C) result also verified the generation of polyester based on the appearance of carbonyl absorption at 1731 cm^{-1} from ester bond. The disappearance of the epoxide group absorption at 910 cm^{-1} while remaining the typical stretching **C−O−C** absorption at 1112 cm^{-1} from OEG also indicated the ring-opening incorporation of the ME_2MO into the polyester backbone (Figures 1C, S3 in the Supporting Information). The successful preparations of the polyesters were also confirmed by the GPC analyses, as shown in Figure 2. The unimodel peaks with low-molecular-weight distribution were clearly observed, which may be explained by the living character of the anionic ring-opening polymerization of PGA and ME_2MO monomers catalyzed by AIP.[33] It should be noted that the M_n measured by GPC is relatively lower than that measured by ^{1}H NMR due to the structural difference between the resultant polyesters and monodispersed polystyrene standards, which were used to generate the calibration curve in GPC analyses.

Figure 3 shows DSC thermograms of the polyesters. The glass-transition temperatures (T_g) of the polyesters were obtained from the DSC curves and listed in Table 2. The T_g exhibited a slight increase from −5.0 to −4.7 °C with the increased degree of

Table 2. Properties of P(PGA-*co*-ME_2MO) Alternating Polyesters

polyester	CMC (10^{-3} g L^{-1})	R_h (nm) at 25 °C	T_g (°C)[a]	DLC%[b]	DLE%[b]	DLC%[c]	DLE%[c]
P(PGA-*co*-ME_2MO)$_{23}$	48.1	100 ± 3.8	−5.0	25.7	34.5	32.6	48.4
P(PGA-*co*-ME_2MO)$_{47}$	9.55	40.2 ± 4.7	−4.7	27.0	37.1	33.8	51.1

[a] Determined by DSC. [b] Rifampin loading properties. [c] DOX loading properties.

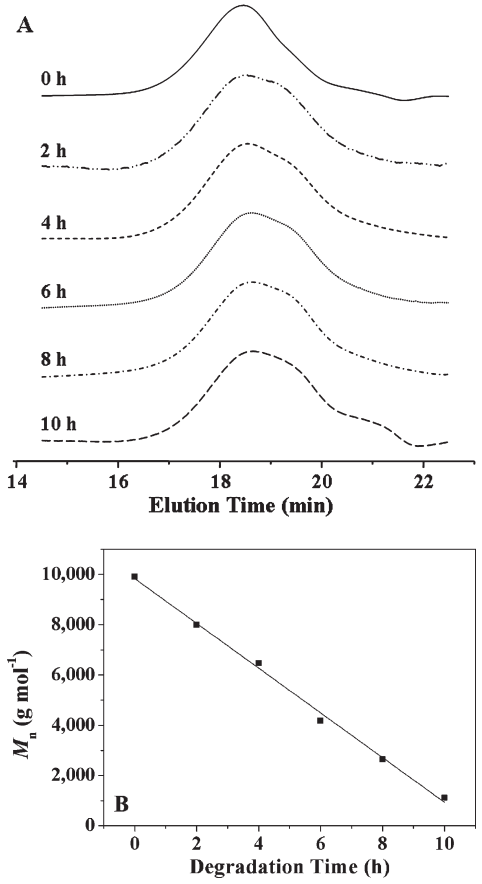

Figure 4. GPC chromatograms of P(PGA-*co*-ME_2MO)$_{47}$ at different degradation times cultured at 37 °C in CPBS (pH 7.4) with 2 μg mL^{-1} (0.08 U mL^{-1}) proteinase K (A) and molecular weights of P(PGA-*co*-ME_2MO)$_{47}$ as a function of degradation time (B).

polymerization (DP) from 23 to 47. This result was consistent with the previous reports and could be commonly described by equation: $T_g(N) = T_g(\infty) - C/N$, where N is the degree of polymerization, $T_g(\infty)$ is the glass-transition temperature for infinity molecular weight, and C is the constant.[15,36]

The in vitro enzymatic degradation of the polyester was carried out at 37 °C in CPBS (pH 7.4) with 2 μg mL^{-1} (0.08 U mL^{-1}) proteinase K.[37] Figure 4 shows the GPC results after incubation for different time intervals. As shown in Figure 4B, the molecular weight (M_n) of incubated polyester decreased significantly with the extension of incubation time. The M_n of polyester quickly dropped to 1100 from 9900 within 10 h at the presence of proteinase K according to GPC analyses. The high degradation rate was mainly attributable to the high surface-to-volume ratio of the polyester micelle, which increased significantly the interaction area between the polyester and proteinase K in the buffer. It indicated that the amphiphilic alternating polyesters can be used in drug delivery system controlled by enzymatic degradation.

Self-Assembly Behavior of P(PGA-*co*-ME_2MO). It was interesting that the obtained polyesters were amphiphilic because of the hydrophobic polyester backbone and the hydrophilic OEG side chains. As shown in Scheme 4, the amphiphilic polyester could form micelles in water. The self-assembly behavior of the polyester in aqueous solution was studied using fluorescence spectroscopy (Figure 5). Pyrene was used as the fluorescence probe, and the CMC was obtained from the plot of fluorescence intensity ratio of I_{335}/I_{332} versus $\log_{10} c$ of the polyester. The CMC values of P(PGA-*co*-ME_2MO)$_{23}$ and P(PGA-*co*-ME_2MO)$_{47}$ were determined to be 4.81×10^{-2} and 9.55×10^{-3} g L^{-1}, respectively (Table 2). The lower CMC value for P(PGA-*co*-ME_2MO)$_{47}$ was probably attributed to the increase in polyester backbone length, which enhanced the probability of polyester backbone winding and the interaction among the polyester chains. This phenomenon also existed in amphiphilic star-shaped copolymer.[38] Figure 5C shows the typical TEM micrograph of (PGA-*co*-ME_2MO)$_{23}$ micelles at 25 °C. The micelles took spherical shape.

Owing to the presence of OEG side chains in the surface, the micelles were assessed to have thermosensitive properties. Dynamic light scattering (DLS) technology was used to determine the thermoinduced size change of the micelles. Figure 6 shows the results of the DLS measurements of the polyester micelles in 0.1 g L^{-1} with temperature ranging from 25 to 60 °C. The hydrodynamic radii (R_h) of the P(PGA-*co*-ME_2MO)$_{23}$ micelles were measured to decrease from 100 nm at 25 °C to 32 nm at 60 °C. The decrease in R_h can be attributed to the rapid hydration-to-dehydration of the OEG chains in the shell with the temperature increase. In contrast, the R_h of P(PGA-*co*-ME_2MO)$_{47}$ micelles was only changed from 40 nm at 25 °C to 23 nm at 60 °C. The lower degree of R_h variation toward P(PGA-*co*-ME_2MO)$_{47}$ micelles may be due to the longer hydrophobic chains in P(PGA-*co*-ME_2MO)$_{47}$, which form more compact hydrophobic cores in the micelles. Therefore, these micelles can be used as stable drug carriers that undergo thermo-induced size decrease without intermicellar aggregation.

In Vitro Cytotoxicity of P(PGA-*co*-ME_2MO). The in vitro cytotoxicities of P(PGA-*co*-ME_2MO)$_{23}$ and P(PGA-*co*-ME_2MO)$_{47}$ toward HeLa cells were evaluated using MTT assay. The sodium dodecyl sulfonate (SDS) was used as the positive control. As shown in Figure 7, the cell viability was treated with polyesters at different concentrations for 24 h. It was observed that the viabilities of HeLa cells were ~85 to 100% at all test concentrations up to 100 mg L^{-1}, revealing the low toxicity and good compatibility of the polyesters to cells.

Drug Loading and Release. To test the possible use of this kind of micelles as drug carriers, rifampin, a bactericidal antibiotic drug, was loaded into the micelles (Scheme 4) and the release behaviors were studied. As listed in Table 2, the DLC% was 25.7 and 27.0%, depending on the compositions of polyesters, whereas the DLE% was 34.5 and 37.1% for P(PGA-*co*-ME_2MO)$_{23}$ and P(PGA-*co*-ME_2MO)$_{47}$ micelles, respectively. The rifampin release behaviors were first studied in CPBS at pH 7.4, 37 °C, and the results were shown in Figure 8. It was interesting to note that the rifampin release from the micelles followed an approximately zero-order kinetic,

Scheme 4. Schematic Illustration of Micellization and Drug-Loading Procedure of Polyester

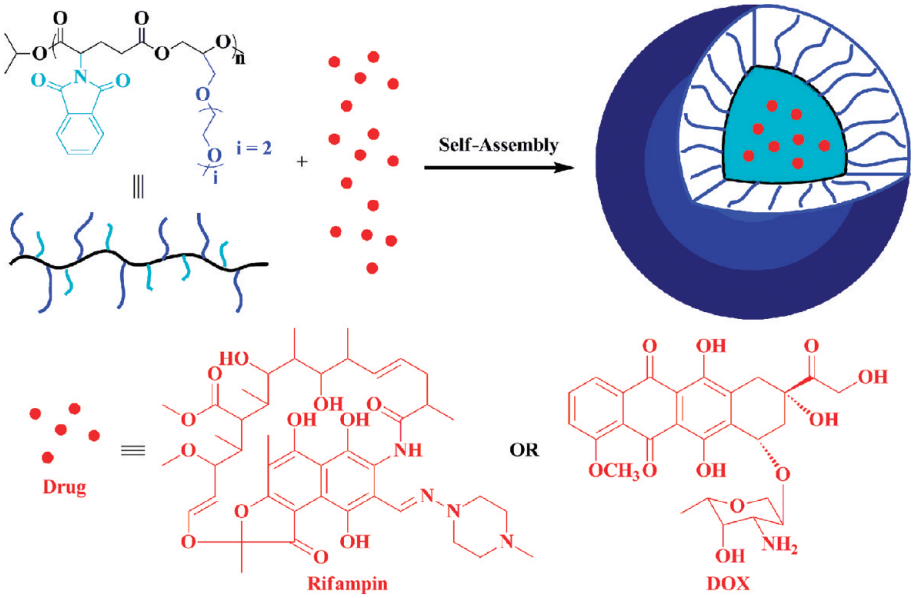

which was attractive for controlled drug release.[39−41] This should be ascribed to the hydrophobic interaction between rifampin and *N*-phthaloyl groups and the compact structure of the micelles at 37 °C. The hydrophobic interaction and compact structure also led to lower degree of rifampin released from the micelles (<25%). In addition, the polyester structure was found to be correlative to the drug release kinetics. P(PGA-*co*-ME_2MO)$_{47}$ micelles exhibited fewer rifampin release than P(PGA-*co*-ME_2MO)$_{23}$ micelles because of the more compact hydrophobic cores in P(PGA-*co*-ME_2MO)$_{47}$ micelles.

In addition, we further investigated the rifampin release in vitro at pH 5.5 or in the presence of proteinase K at pH 7.4. P(PGA-*co*-ME_2MO)$_{47}$ micelles were used in this study for their relatively stability at pH 7.4 without enzyme, from which only 10% of the loaded rifampin was released in the test duration (30 h). As shown in Figure 8, the rifampin releases were accelerated at pH 5.5 or in the presence of proteinase K at pH 7.4. The release behaviors both adopted zero-order kinetics for up to 12 h. It was also observed that the cumulative release of the rifampin can reach almost 100% under the presence of proteinase K, which was much higher than that at pH 7.4 (10%) or pH 5.5 (40%) without enzyme. This should be attributed to the presence of proteinase K, which can cause effective degradation of the polyester backbone (Figure 4).[37] GPC analyses were used to verify the degradation of the polyester under these conditions. As shown in Figure S4 (Supporting Information), the polyester was stable in CPBS at pH 7.4 after performing rifampin release for 30 h. The lower pH (pH 5.5) and the presence of proteinase K (2 μg mL^{-1}, 0.08 U mL^{-1}) will partially lead to degradation of the polyester, demonstrated by the GPC as decrease in the M_n and broadening of PDI. So, accelerated drug release rate and increased drug release amount could be observed in these conditions as compared with that at pH 7.4 without enzyme. On the basis of the aforementioned data, we can conclude that these novel amphiphilic alternating polyesters are of great potential use as smart drug carriers, which are stable under physiological condition and can undergo sustained release at the targeted sites with stimulus, such as lower pH or enzyme.

To confirm the release behaviors and for further application, we loaded DOX, an anticancer drug, into the micelles (Scheme 4), and the release behaviors were also studied. The DLC% were 32.6 and 33.8%, whereas the DLE% were 48.4 and 51.1% for P(PGA-*co*-ME_2MO)$_{23}$ and P(PGA-*co*-ME_2MO)$_{47}$ micelles, respectively. The DLC% and DLE% of DOX was somewhat higher than that of rifampin because of the lower molecular weight of DOX and the chemical structure difference. In a similar way as rifampin, the cumulative release of the DOX can reach almost 100% under the presence of proteinase K, whereas lower release was observed at either pH 7.4 (10%) or pH 5.5 (40%) without enzyme in the test duration (72 h) (Figure 9). These release profiles are beneficial not only for minimizing drug loss in blood but also for selective accumulation in tumor tissue by the EPR effect, which may enhance the overall therapeutic efficacy in vivo relative to free DOX.

Intracellular DOX Release. The cellular uptake and intracellular release behaviors of DOX-loaded polyester micelles toward HeLa cells were monitored by CLSM. The HeLa cells were incubated with DOX-loaded micelles for 0.5 or 2 h with free DOX as the control (10 mg L^{-1} DOX). As shown in Figure 10A−C, results showed stronger DOX fluorescence in the cells after 0.5 h incubated with free DOX than DOX-loaded polyester micelles, indicating fast internalization of free DOX. With the incubation time increased to 2 h, stronger DOX fluorescence was observed in the cells incubated with DOX-loaded polyester micelles (Figure 10D−F). It has been reported that the incorporation of DOX in the hydrophobic cores of micelles decreases the DOX fluorescence intensity compared with free DOX at the same concentration because of the self-quenching effect of DOX.[42,43] Therefore, the enhanced fluorescence intensity should be the result of the high endocytosis efficiency of DOX-loaded polyester micelles and enhanced intracellular release of DOX with the micelles degradation in HeLa cells. It is worth noting that the DOX fluorescence is stronger in the cells incubated with DOX-loaded P(PGA-*co*-ME_2MO)$_{23}$ micelles than with DOX-loaded P(PGA-*co*-ME_2MO)$_{47}$ micelles. This is because the DOX release from DOX-loaded P(PGA-*co*-ME_2MO)$_{23}$ micelles is quicker (as shown in Figure 9).

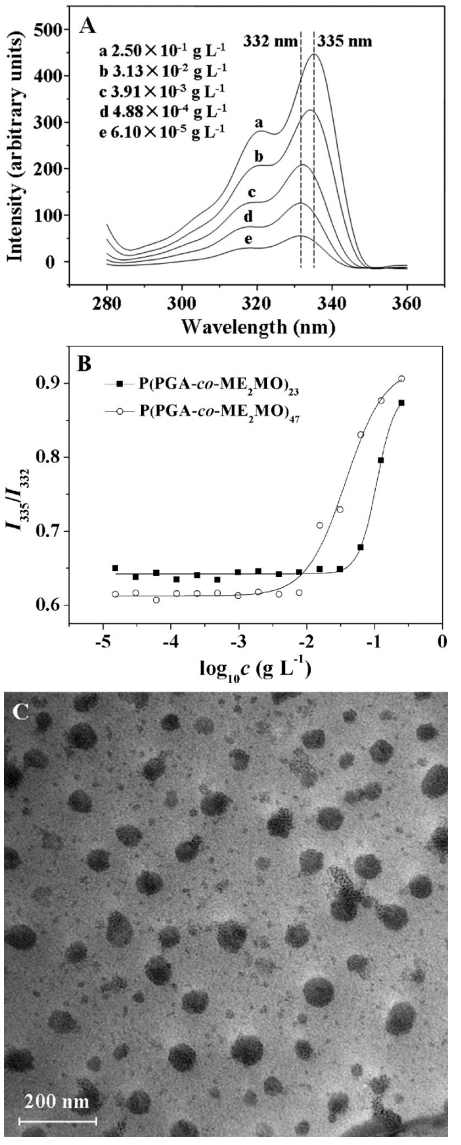

Figure 5. Excitation spectra of pyrene in aqueous solution of P(PGA-*co*-$ME_2MO)_{23}$ at different concentrations (λ_{em} = 390 nm) (A), the intensity ratio (I_{335}/I_{332}) as a function of concentration (B), and typical TEM micrograph of P(PGA-*co*-$ME_2MO)_{23}$ (C).

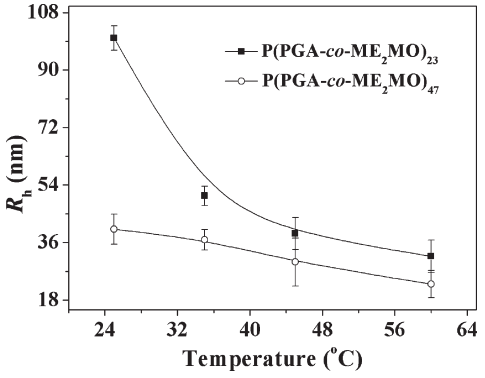

Figure 6. Hydrodynamic radii (R_h) of P(PGA-*co*-ME_2MO) in aqueous solution as a function of temperature.

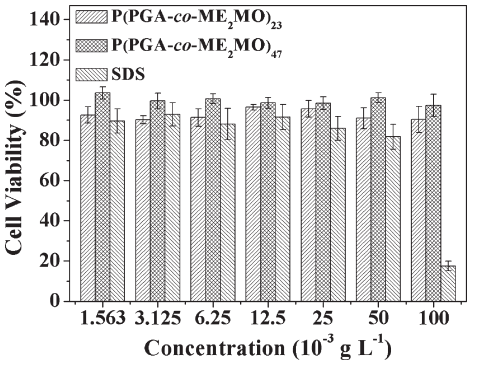

Figure 7. In vitro cytotoxicity of P(PGA-*co*-ME_2MO) to HeLa cells with SDS as the positive control. Data were presented as the average ± standard deviation (n = 3).

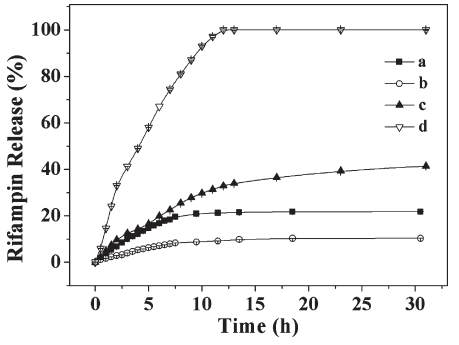

Figure 8. Release profiles of rifampin from rifampin-loaded P(PGA-*co*-$ME_2MO)_{23}$ micelles in CPBS at 37 °C, pH 7.4 (a), and P(PGA-*co*-$ME_2MO)_{47}$ micelles in CPBS at 37 °C, pH 7.4 (b), pH 5.5 (c), and pH 7.4 with 2 μg mL^{-1} (0.08 U mL^{-1}) proteinase K (d).

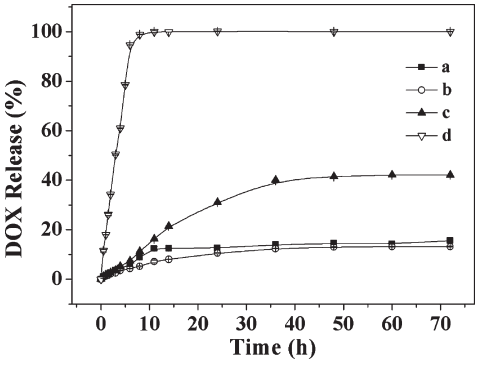

Figure 9. Release profiles of DOX from DOX-loaded P(PGA-*co*-$ME_2MO)_{23}$ micelles in CPBS at 37 °C, pH 7.4 (a), and P(PGA-*co*-$ME_2MO)_{47}$ micelles in CPBS at 37 °C, pH 7.4 (b), pH 5.5 (c), and pH 7.4 with 2 μg mL^{-1} (0.08 U mL^{-1}) proteinase K (d).

In Vitro Activity of DOX-Loaded P(PGA-*co*-ME_2MO) Micelles. As discussed above, the DOX-free polyester micelles showed no noticeable cytotoxicities up to 100 mg L^{-1} (Figure 7). In vitro activity of free DOX and DOX-loaded polyester micelles for HeLa cells was estimated. As shown in Figure 11, DOX-loaded polyester micelles showed more effective inhibitory effect on the proliferation of cancer cells compared with the free DOX. The higher toxicity of DOX-loaded polyester micelles (IC_{50} = 3.28, 3.42 mg L^{-1} for

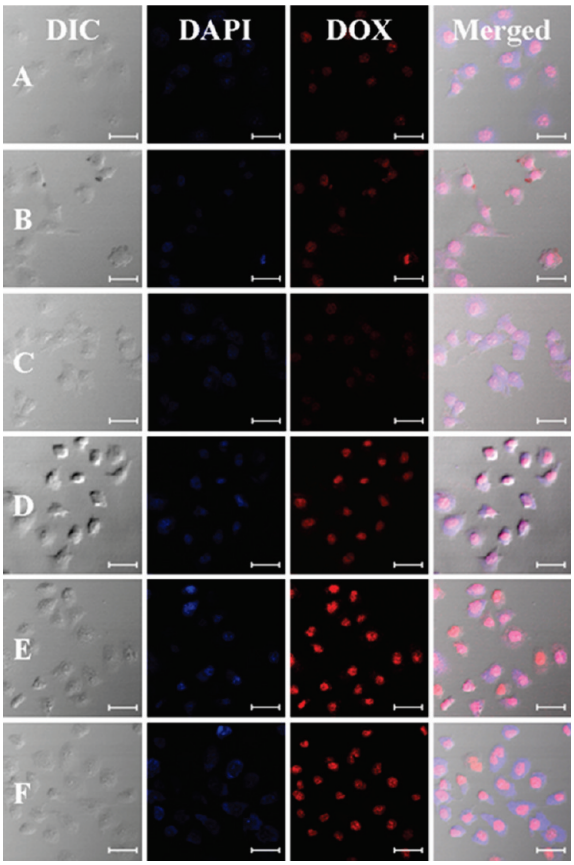

Figure 10. Representative CLSM images of HeLa cells incubated with free DOX and DOX-loaded micelles: 0.5 h, incubated with free DOX (A); 0.5 h, incubated with DOX-loaded P(PGA-*co*-$ME_2MO)_{23}$ micelles (B); 0.5 h, incubated with DOX-loaded P(PGA-*co*-$ME_2MO)_{47}$ micelles (C); 2 h, incubated with free DOX (D); 2 h, incubated with DOX-loaded P(PGA-*co*-$ME_2MO)_{23}$ micelles (E); 2 h, incubated with DOX-loaded P(PGA-*co*-$ME_2MO)_{47}$ micelles (F). For each panel, the images from left to right show differential interference contrast (DIC) image, cell nuclei stained by DAPI (blue), DOX fluorescence in cells (red), and overlays of the three images. The bar represents 40 μm.

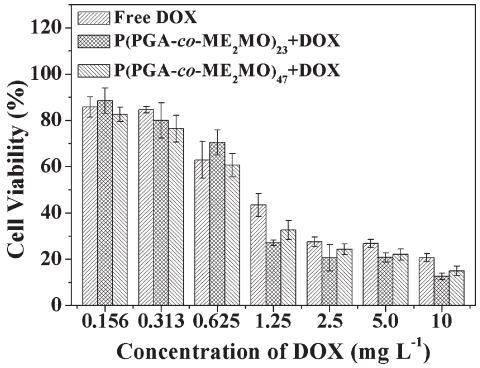

Figure 11. In vitro cytotoxicity of DOX-loaded polyester micelle to HeLa cells with free DOX as the control. Data were presented as the average ± standard deviation (n = 3).

P(PGA-*co*-$ME_2MO)_{23}$, P(PGA-*co*-$ME_2MO)_{47}$ micelles, respectively) compared with free DOX (IC_{50} = 3.79 mg L^{-1}) was probably due to the effective endocytosis and quick intracellular DOX release within the endosomes.

CONCLUSIONS

Novel amphiphilic P(PGA-*co*-ME_2MO) polyesters with pendent OEG chains were prepared by alternating ROP of PGA and ME_2MO monomers. The synthesized polyesters were verified to have precise alternating structure and amphiphilic properties. They can form micelles in the aqueous solution with hydrophobic polyester backbone cores and thermosensitive OEG shells. The micelles underwent thermoinduced R_h decrease to form compact micelles without intermicellar aggregation. Rifampin and DOX were loaded into the compact micelles. The sustained zero-order release was observed in the test duration at pH 7.4, 37 °C. However, the cumulative release of drug from the micelles was relatively low. In particular, for P(PGA-*co*-$ME_2MO)_{47}$ micelles, only 10% of the drug can be release from micelles. Fortunately, the sustained release rate can be accelerated at lower pH 5.5 or in the presence of proteinase K at pH 7.4 due to the degradation of the polyesters under these conditions. The in vitro cell experiments revealed that these polyester micelles accomplished fast release of DOX inside cells and higher anticancer efficacy as compared with the free DOX control. Therefore, it is believed that this kind of polyesters may hold vast potential for controlled drug delivery systems, which show stability under physiological condition and accelerated release at the targeting sites (e.g., low pH or enzyme presence).

ASSOCIATED CONTENT

Supporting Information. ^{1}H NMR and FT-IR spectra of monomers and GPC chromatograms of polyester after rifampin release. This material is available free of charge via the Internet at http://pubs.acs.org.

AUTHOR INFORMATION

Corresponding Author

*E-mail: zhuangxl@ciac.jl.cn.

Author Contributions

§These two authors are joint first authors.

ACKNOWLEDGMENT

This work was supported by grants from National Natural Science Foundation of China (Key Project 50733003, Project 20904053 and 50973108, A3 Foresight Program 50425309), Program of Scientific Development of Jilin Province (20090135), and Knowledge Innovation Program of the Chinese Academy of Sciences (Grant No. KJCX2-YW-H19). We would like to thank Ms. Lili Ma from Changchun Institute of Applied Chemisty for her help with the polymer characterization.

REFERENCES

(1) Gaucher, G.; Satturwar, P.; Jones, M. C.; Furtos, A.; Leroux, J. C. *Eur. J. Pharm. Biopharm.* **2010**, *76*, 147–158.
(2) Li, C. H.; Ge, Z. S.; Fang, J.; Liu, S. Y. *Macromolecules* **2009**, *42*, 2916–2924.
(3) Lao, S. B.; Zhang, Z. X.; Xu, H. H.; Jiang, G. B. *Carbohydr. Polym.* **2010**, *82*, 1136–1142.
(4) Petersen, M. A.; Yin, L. G.; Kokkoli, E.; Hillmyer, M. A. *Polym. Chem.* **2010**, *1*, 1281–1290.
(5) Wan, W. M.; Pan, C. Y. *Polym. Chem.* **2010**, *1*, 1475–1484.
(6) Liu, G. Y.; Hu, X. F.; Chen, C. J.; Ji, J. A. *J. Appl. Polym. Sci.* **2010**, *118*, 3197–3202.

(7) Wang, C.; Chen, Q. S.; Xu, H. P.; Wang, Z. Q.; Zhang, X. *Adv. Mater.* **2010**, *22*, 2553–2555.
(8) Liu, Z. H.; Tian, Y. M.; Sun, F.; Meng, F. Y.; Zheng, Y. H.; Jiang, F. M. *Colloids Surf., A* **2008**, *318*, 122–124.
(9) Chen, X. J.; Sanchez-Gaytan, B. L.; Hayik, S. E. N.; Fryd, M.; Wayland, B. B.; Park, S. J. *Small* **2010**, *6*, 2256–2260.
(10) Easwaramoorthi, S.; Kim, P.; Lim, J. M.; Song, S.; Suh, H.; Sessler, J. L.; Kim, D. *J. Mater. Chem.* **2010**, *20*, 9684–9694.
(11) Hung, S. C.; Shiu, S. C.; Chao, J. J.; Lin, C. F. *J. Electrochem. Soc.* **2010**, *157*, D496–D499.
(12) Savariar, E. N.; Aathimanikandan, S. V.; Thayumanavan, S. *J. Am. Chem. Soc.* **2006**, *128*, 16224–16230.
(13) Li, Y. G.; Zhang, Y. Q.; Yang, D.; Li, Y. J.; Hu, J. H.; Feng, C.; Zhai, S. J.; Lu, G. L.; Huang, X. Y. *Macromolecules* **2010**, *43*, 262–270.
(14) Ding, J. X.; Xiao, C. S.; Tang, Z. H.; Zhuang, X. L.; Chen, X. S. *Macromol. Biosci.* **2011**, *11*, 192–198.
(15) Ding, J. X.; Xiao, C. S.; Zhao, L.; Cheng, Y. L.; Ma, L. L.; Tang, Z. H.; Zhuang, X. L.; Chen, X. S. *J. Polym. Sci., Part A: Polym. Chem.* **2011**, *49*, 2665–2676.
(16) Qiu, S.; Huang, H.; Dai, X. H.; Zhou, W.; Dong, C. M. *J. Polym. Sci., Part A: Polym. Chem.* **2009**, *47*, 2009–2023.
(17) Gou, P. F.; Zhu, W. P.; Shen, Z. Q. *Polym. Chem.* **2010**, *1*, 1205–1214.
(18) Elfinger, M.; Pfeifer, C.; Uezguen, S.; Golas, M. M.; Sander, B.; Maucksch, C.; Stark, H.; Aneja, M. K.; Rudolph, C. *Biomacromolecules* **2009**, *10*, 2912–2920.
(19) Heath, F.; Saeed, A. O.; Pennadam, S. S.; Thurecht, K. J.; Alexander, C. *Polym. Chem.* **2010**, *1*, 1252–1262.
(20) Konda, M.; Kimura, Y. *Sen'i Gakkaishi* **2003**, *59*, 319–323.
(21) Hiltunen, K.; Seppala, J. V.; Itavaara, M.; Harkonen, M. *J. Environ. Polym. Degrad.* **1997**, *5*, 167–173.
(22) Duong, H. T. T.; Nguyen, T. L. U.; Stenzel, M. H. *Polym. Chem.* **2010**, *1*, 171–182.
(23) Van der Ende, A. E.; Sathiyakumar, V.; Diaz, R.; Hallahan, D. E.; Harth, E. *Polym. Chem.* **2010**, *1*, 93–96.
(24) Taghdisi, S. M.; Abnous, K.; Mosaffa, F.; Behravan, J. *J. Drug Targeting* **2010**, *18*, 277–281.
(25) Choi, J. H.; Jang, J. Y.; Joung, Y. K.; Kwon, M. H.; Park, K. D. *J. Controlled Release* **2010**, *147*, 420–427.
(26) Du, Y. Z.; Weng, Q.; Yuan, H.; Hu, F. Q. *ACS Nano* **2010**, *4*, 6894–6902.
(27) Guo, M. A.; Que, C. L.; Wang, C. H.; Liu, X. Z.; Yan, H. S.; Liu, K. L. *Biomaterials* **2011**, *32*, 185–194.
(28) Mikhail, A. S.; Allen, C. *Biomacromolecules* **2010**, *11*, 1273–1280.
(29) Janib, S. M.; Moses, A. S.; MacKay, J. A. *Adv. Drug Delivery Rev.* **2010**, *62*, 1052–1063.
(30) Lutz, J. F. *J. Polym. Sci., Part A: Polym. Chem.* **2008**, *46*, 3459–3470.
(31) Qiao, Z. Y.; Du, F. S.; Zhang, R.; Liang, D. H.; Li, Z. C. *Macromolecules* **2010**, *43*, 6485–6494.
(32) Feng, L.; Hao, J. Y.; Xiong, C. D.; Deng, X. M. *Chem. Commun.* **2009**, 4411–4413.
(33) Albertsson, A. C.; Varma, I. K. *Biomacromolecules* **2003**, *4*, 1466–1486.
(34) Wang, Y. C.; Shen, S. Y.; Wu, Q. P.; Chen, D. P.; Wang, J.; Steinhoff, G.; Ma, N. *Macromolecules* **2006**, *39*, 8992–8998.
(35) Tipson, R. S. *J. Org. Chem.* **1956**, *21*, 1353–1357.
(36) Odriscoll, K.; Sanayei, R. A. *Macromolecules* **1991**, *24*, 4479–4480.
(37) Zeng, J.; Chen, X. S.; Liang, Q. Z.; Xu, X. L.; Jing, X. B. *Macromol. Biosci.* **2004**, *4*, 1118–1125.
(38) Cheng, J.; Ding, J. X.; Wang, Y. C.; Wang, J. *Polymer* **2008**, *49*, 4784–4790.
(39) Hu, Y.; Jiang, X. Q.; Ding, Y.; Zhang, L. Y.; Yang, C. Z.; Zhang, J. F.; Chen, J. N.; Yang, Y. H. *Biomaterials* **2003**, *24*, 2395–2404.
(40) Li, X.; Wu, Q.; Lu, M.; Zhang, F.; Lin, X. F. *J. Polym. Sci., Part A: Polym. Chem.* **2008**, *46*, 2734–2744.
(41) Liu, H. B.; Farrell, S.; Uhrich, K. *J. Controlled Release* **2000**, *68*, 167–174.
(42) Sun, H. L.; Guo, B. N.; Li, X. Q.; Cheng, R.; Meng, F. H.; Liu, H. Y.; Zhong, Z. Y. *Biomacromolecules* **2010**, *11*, 848–854.
(43) Wang, Y. C.; Li, Y.; Sun, T. M.; Xiong, M. H.; Wu, J. A.; Yang, Y. Y.; Wang, J. *Macromol. Rapid Commun.* **2010**, *31*, 1201–1206.